Report

Cell Reports

A Switch in Thermal Preference in *Drosophila* Larvae Depends on Multiple Rhodopsins

Graphical Abstract

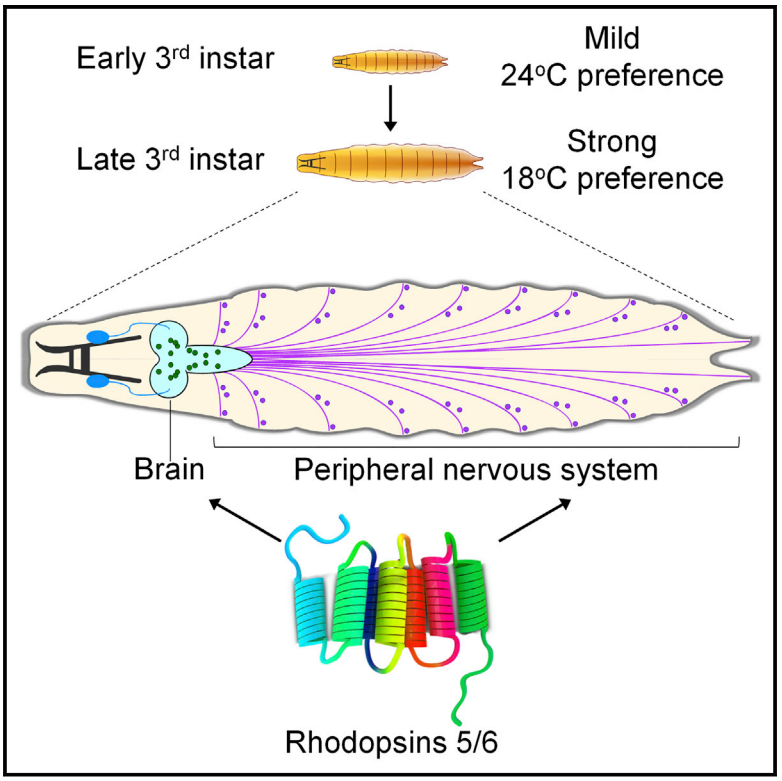

Authors

Takaaki Sokabe, Hsiang-Chin Chen, Junjie Luo, Craig Montell

Correspondence

craig.montell@lifesci.ucsb.edu

In Brief

Sensing optimal temperatures contributes to animal survival. Sokabe et al. reveal an unconventional role for two rhodopsins that function in the *Drosophila* brain and in body wall neurons to cause an age-specific switch in thermal preference.

Highlights

- *Drosophila* larvae undergo age-dependent transitions in temperature selection
- Temperature selection in mid- and late-third-instar larvae depends on *rh5* and *rh6*
- *rh5* and *rh6* are required in *trpA1*-positive neurons in the brain and the periphery
- Rh5 and Rh6 function in thermotaxis through a Gq/PLC/TRPA1 signaling cascade

Sokabe et al., 2016, Cell Reports *17*, 336–344
October 4, 2016
http://dx.doi.org/10.1016/j.celrep.2016.09.028

OPEN ACCESS
CellPress

Cell Reports
Report

A Switch in Thermal Preference in *Drosophila* Larvae Depends on Multiple Rhodopsins

Takaaki Sokabe,[1,3] Hsiang-Chin Chen,[1,3] Junjie Luo,[1,2] and Craig Montell[1,4,*]
[1]Neuroscience Research Institute and Department of Molecular, Cellular and Developmental Biology, University of California, Santa Barbara, Santa Barbara, CA 93106, USA
[2]Department of Biological Chemistry, The Johns Hopkins University School of Medicine, Baltimore, MD 21205, USA
[3]Co-first author
[4]Lead Contact
*Correspondence: craig.montell@lifesci.ucsb.edu
http://dx.doi.org/10.1016/j.celrep.2016.09.028

SUMMARY

Drosophila **third-instar larvae exhibit changes in their behavioral responses to gravity and food as they transition from feeding to wandering stages. Using a thermal gradient encompassing the comfortable range (18°C to 28°C), we found that third-instar larvae exhibit a dramatic shift in thermal preference. Early third-instar larvae prefer 24°C, which switches to increasingly stronger biases for 18°C–19°C in mid- and late-third-instar larvae. Mutations eliminating either of two rhodopsins, Rh5 and Rh6, wiped out these age-dependent changes in thermal preference. In larvae, Rh5 and Rh6 are thought to function exclusively in the light-sensing Bolwig organ. However, the Bolwig organ was dispensable for the thermal preference. Rather, Rh5 and Rh6 were required in *trpA1*-expressing neurons in the brain, ventral nerve cord, and body wall. Because Rh1 contributes to thermal selection in the comfortable range during the early to mid-third-instar stage, fine thermal discrimination depends on multiple rhodopsins.**

INTRODUCTION

The capacity to sense and avoid acute exposure to noxious heat and cold is critical for survival, and in many animals, this ability depends on direct activation of transient receptor potential (TRP) channels (Julius, 2013; Venkatachalam and Montell, 2007). Animals ranging from worms to humans are sensitive to small temperature differences in the comfortable range and respond by selecting their preferred temperature zones (Julius, 2013; Venkatachalam et al., 2014; Venkatachalam and Montell, 2007). This behavior is especially acute in poikilothermic organisms such as the fruit fly, *Drosophila melanogaster*, which equilibrates its body temperature with the environment. As a consequence, *Drosophila* can respond behaviorally to thermal fluctuations of a fraction of a degree (Fowler and Montell, 2013; Klein et al., 2015). This is best documented in *Drosophila* larvae (Klein et al., 2015), and we have shown previously that the exquisite sensitivity to small changes in temperature in the comfortable range depends on a thermosensory signaling cascade that is initiated by one of the seven rhodopsins (Rh1) (Kwon et al., 2008; Shen et al., 2011).

The third-instar larval stage is a period characterized by dynamic modifications in behavior. Early to mid-third-instar larvae are motivated by feeding, while the late-third-instar larvae must also prepare for the final, wandering stage, when they escape from food and subsequently pupate. Due to these changing needs, third-instar larvae transition from positive to negative geotaxis. In addition, attraction to food switches to aversion during third-instar larvae (Wu et al., 2003). However, it was unclear whether third-instar larvae also exhibit major changes in thermal preference before entering the wandering stage.

In this study, using a linear 18°C–28°C thermal gradient, we established that third-instar larvae underwent a dramatic shift in their thermal preference over the course of 48 hr. Early third-instar larvae had a preference for 24°C, while mid-third-instar larvae had a bias for 18°C. By the late-third-instar period, immediately preceding the wandering stage, the animals strongly favored 18°C. Surprisingly, temperature selection in late-third-instar larvae was normal in mutants missing Rh1, which we previously found was required in mid-third-instar larvae (Shen et al., 2011). Instead, two other rhodopsins, Rh5 and Rh6, were strictly required in late-third-instar larvae for choosing 18°C. These two rhodopsins functioned in neurons in the brain and body wall. Thus, the age-dependent change in thermal preference depended on a thermal detection system consisting of multiple rhodopsins as critical components.

RESULTS

Changes in Temperature Preference in Third-Instar Larvae

In order to clarify the thermal behavior of larvae, we devised an apparatus that allowed the animals to choose their preferred temperature within a continuous linear gradient (Figures 1A–1C). We focused on the 18°C–28°C range, since this included the temperatures that support the most robust growth and survival during the larval period. Furthermore, we restricted the temperatures to 18°C or higher, since, at lower temperatures, larval locomotion was compromised. To characterize changes

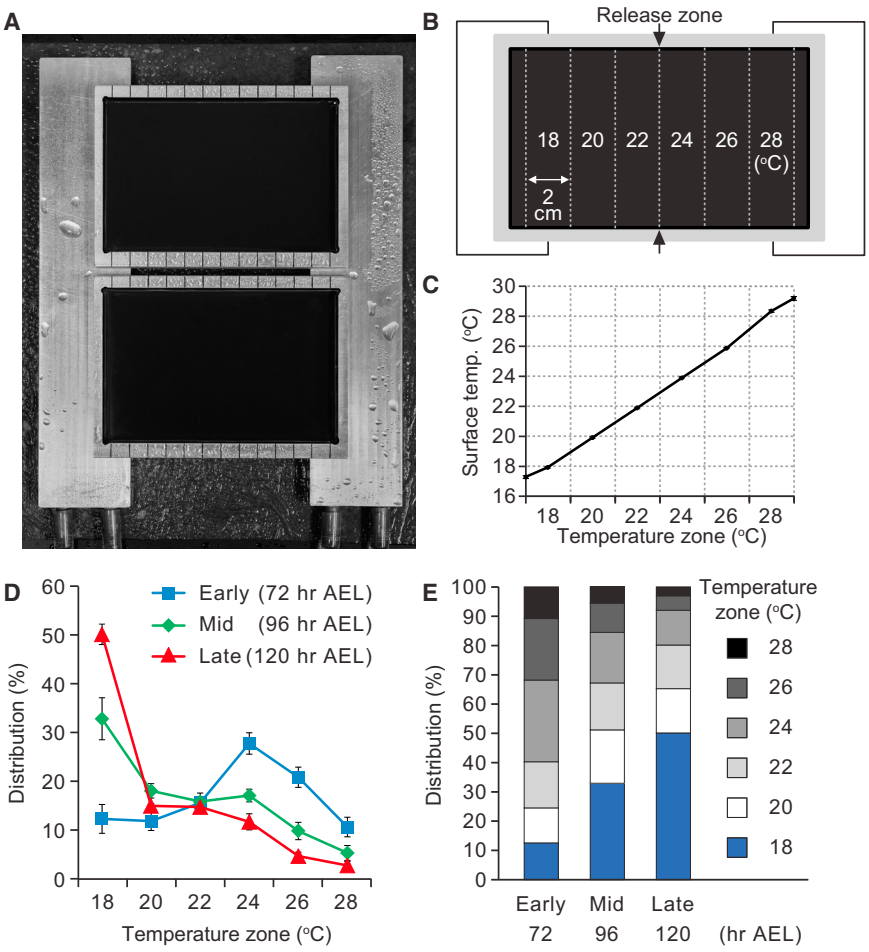

Figure 1. Age-Dependent Changes in Thermal Preference in Third-Instar Larvae

(A) Apparatus for assaying thermal preference using a temperature gradient. The sides of the test plates are placed on aluminum blocks, each of which is set at a distinct temperature using circulating water from a bath.

(B) Schematic diagram of a test plate divided into 2-cm wide zones. 10–20 min after releasing the larvae between the 22°C and 24°C zones, the number of larvae in each of the six zones was tabulated.

(C) Actual temperatures measured in the center of the zones. Data represent mean ± SD. n = 7.

(D and E) Mean percentages of control (w^{1118}) early-, mid-, and late-stage third-instar larvae in the six zones that constitute the 18°C–28°C temperature gradient. n = 6–7 experiments. The error bars in (D) represent ±SEM.

See also Figure S1.

in thermal preferences in early, mid-, and late-third-instar larvae, we collected control (w^{1118}) larvae at 72, 96, and 120 hr after egg laying (AEL), respectively. 72 hr AEL coincided with the initiation of the third-instar larval period, while 120 hr AEL was immediately prior to the wandering stage when the larvae climb out of food-containing environments and initiate pupation. We did not characterize the wandering larvae (>120 hr AEL), due to their strong motivation to scale the edges of the gradient plate, thereby precluding a reliable analysis of their thermal preference.

We released the larvae in the border between 22°C and 24°C zones (Figure 1B) and allowed the animals to explore the thermal landscape for 10–20 min, depending on the stage. Then, we determined the distribution of the animals within the six temperature zones (Figures 1B and 1C). We found that third-instar larvae exhibited a striking shift in their preferred temperature as the animals aged between 72 and 120 hr AEL. The early third-instar larvae chose the 24°C zone at the highest frequency (27.9% ± 2.2%), and there was virtually no bias for one extreme of the temperature gradient over the other (Figures 1D and 1E; 18°C, 12.5% ± 2.9%; 28°C, 10.8% ± 2.0%). 24 hr later, the mid-third-instar larvae altered their temperature preferences significantly. These larvae selected 18°C at the highest frequency (Figures 1D and 1E; 18°C, 32.9% ± 4.3%), consistent with the two-way choice assays (Kwon et al., 2008). The late-third-instar larvae displayed a strong preference for 18°C, and temperatures higher than 24°C became highly aversive (Figures 1D and 1E; 18°C, 50.2% ± 2.1%; 28°C, 3.0% ± 0.8%). In contrast to the early third-instar larvae, the late third-instar larvae favored the 18°C over the 28°C zone ~17-fold.

The late third-instar larvae were at a stage just prior to when wandering larvae begin climbing up surfaces to escape from food in preparation for pupation. Therefore, to test whether the strong selection of the 18°C zone was influenced by the juxtaposition of this zone near the edge of the plate, we created a temperature gradient in which the 18°C zone was in the center, and the warmer zones radiated out bisymmetrically on both sides (Figure S1A). We found that the late third-instar larvae still favored the 18°C zone (Figures S1B and S1C). These results indicated that third-instar larvae changed their temperature preferences in an age-dependent manner over the course of 48 hr and selected the lower temperature within the comfortable range as they got older.

Requirements for Multiple Rhodopsins for Transitions in Temperature Selection

We reported previously that Rh1 was required in third-instar larvae for choosing 18°C over other temperatures in the comfortable range (19°C–24°C) (Shen et al., 2011). Due to the significant changes in temperature preference during the third-instar period, we rechecked *rh1* null ($ninaE^{I17}$) larvae and found that $ninaE^{I17}$ larvae at the mid-third-instar stage (96 hr AEL) were impaired in 18°C selection, consistent with previous results (Figure S2A) (Shen et al., 2011). At 96 hr, the $ninaE^{I17}$ mutant animals slightly favored the 24°C and 26°C zones and exhibited a

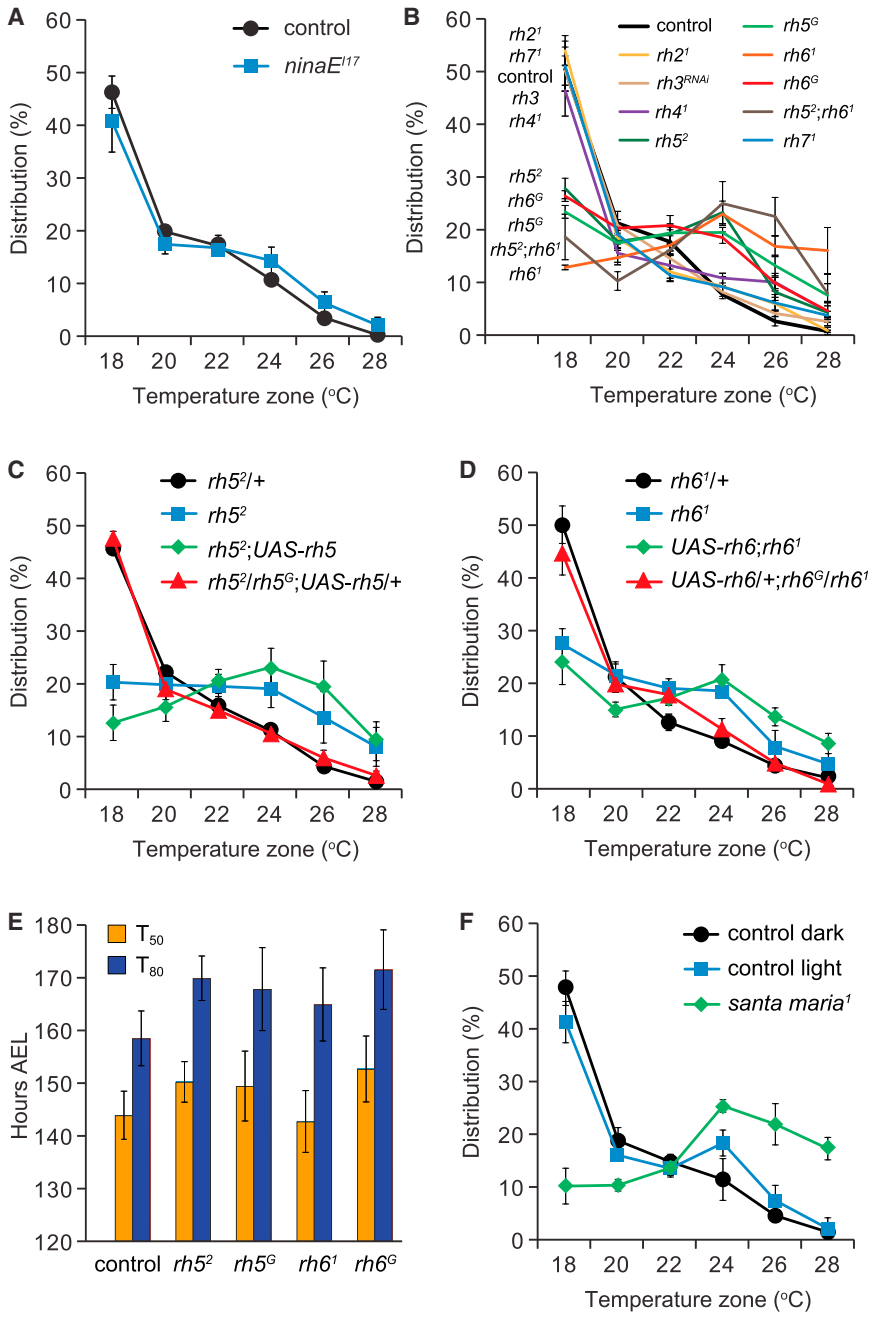

Figure 2. Requirements for *rh5* and *rh6* in Late-Third-Instar Larvae for Selecting the Optimal Temperature

(A–D and F) Distribution of late-third-instar larvae (120 hr AEL) of the indicated genotypes over 18°C–28°C continuous thermal gradients.

(A) Control (w^{1118}) and *rh1* null mutant ($ninaE^{I17}$). n = 4–5.

(B) Rhodopsin mutants were used, with the exception of RNAi-mediated knockdown of *rh3*, which was performed using *dicer2;;elav-GAL4/UAS-rh3*^{RNAi}. n = 3–5.

(C) Testing for rescue of the *rh5* mutant thermotaxis phenotype by expressing wild-type *UAS-rh5* under the control of the *GAL4* knocked into the *rh5* locus ($rh5^G$). n = 4–6.

(D) Testing for rescue of the *rh6* mutant phenotype by expressing wild-type *UAS-rh6* under the control of the *GAL4* knocked into the *rh6* locus ($rh6^G$). n = 4–5.

(E) The time to pupation of the indicated genotypes. T_{50} and T_{80} denote the times required for 50% and 80% of larvae to become pupae, respectively. n = 6–9.

(F) Thermal distribution of control flies (w^{1118}) maintained under dark conditions (<0.1 μW/cm^2) or under ambient light (~73 μW/cm^2). The *santa maria*^{1} larvae were tested in the dark. n = 3.

The error bars represent ± SEM. See also Figure S2.

temperature preference similar to control animals at 72 hr AEL (Figures 1D and S2A). We also characterized early third-instar larvae (72 hr AEL) and found that the $ninaE^{I17}$ distribution pattern on the thermal gradient was shifted slightly toward the warmer temperatures (Figure S2B).

Due to the strong 18°C selection by control late third-instar larvae, we tested whether Rh1 was required in these animals. Surprisingly, the distribution pattern of the $ninaE^{I17}$ late third-instar larvae was indistinguishable from that of the controls (Figure 2A). Therefore, we tested whether mutation or RNAi knockdown of any of the other six rhodopsin genes (*rh2–rh7*) impaired 18°C selection. We found that $rh5^2$ and $rh6^1$ mutant larvae displayed severe defects in choosing 18°C (Figure 2B). Other rhodopsin mutants or RNAi knockdown had no impact on thermotactic behavior (Figure 2B). Moreover, the phenotype of $rh5^2;rh6^1$ double-mutant flies was similar to that of the $rh5^2$ and $rh6^1$ single-mutant animals (Figure 2B). During the early- and mid-third-instar larval stages, the $rh2^1$, *rh3* (RNAi knockdown), $rh4^1$, and $rh7^1$ also displayed thermal distribution patterns similar to those of control larvae (Figures S2C and S2D).

We generated second *rh5* and *rh6* alleles, each of which included a *GAL4* reporter inserted at the position of the normal ATG, in place of the N-terminal 540 and 499 base pairs (bp) of *rh5* and *rh6*, respectively ($rh5^G$ and $rh6^G$; Figures S2E and S2F). These *GAL4* reporters were strongly expressed in the Bolwig organ (Figures S2G and S2H), consistent with previous findings that these rhodopsins are produced and function in this light-sensing organ (Sprecher et al., 2007). Both the $rh5^G$ and $rh6^G$ larvae showed defects similar to those of $rh5^2$ and $rh6^1$ during the mid- and late third-instar periods (Figures 2B and S2C). We rescued the $rh5^2$ and $rh6^1$ mutant phenotypes in late third-stage instar with wild-type *rh5* and *rh6* transgenes (*UAS-rh5* and *UAS-rh6*, respectively; Figures 2C and 2D). These *rh5* and *rh6* mutant phenotypes did not appear

to be due to developmental delays, as the time to pupation was indistinguishable between the mutants and controls (Figure 2E). Moreover, based on the morphology of the mouth hooks and spiracles, the percentages of *rh5* and *rh6* mutant larvae that entered the early third-instar larval stage at 74 hr AEL were not significantly different from those of the control (Figure S2I). Thus, we conclude that both Rh5 and Rh6 contributed to thermal preference in the mid- and late-stage third-instar larvae. Due to the strong temperature preference among control late third-instar larvae, we focused the remainder of our study on this larval stage.

Light and the Bolwig Organ Do Not Function in Optimal Temperature Selection

Rhodopsins consist of two subunits: a protein moiety referred to as the opsin and a vitamin A derivative that is the chromophore. To test for a requirement for the chromophore, we assayed the temperature selection of a mutant, *santa maria*^{1}, which disrupts a protein that contributes to retinoid formation (Wang et al., 2007). The *santa maria*^{1} late third-instar larvae were impaired in 18°C selection similar to the *rh5* or *rh6* mutants (Figure 2F). This did not appear to be due to a developmental delay, as *santa maria*^{1} entered the third-instar larvae stage with similar timing as control animals (Figure S2J).

In *Drosophila* photoreceptor cells, the chromophore is required for not only for sensing light but also for translocation of rhodopsin from the endoplasmic reticulum to the plasma membrane (Ozaki et al., 1993). To determine whether light influenced thermotaxis, we performed gradient assays in the presence or absence of light. We found that control larvae displayed the same strong bias for the 18°C zone in the light or dark (Figure 2F). Because thermotaxis is not dependent on light, we suggest that the impairment exhibited by *santa maria*^{1} larvae reflects a requirement for the chromophore for exiting the endoplasmic reticulum (Ozaki et al., 1993).

Rh5 and Rh6 are expressed in the Bolwig organ (Sprecher et al., 2007) (Figure 3A), which is required for light avoidance (Mazzoni et al., 2005). To test whether temperature sensation depended on the Bolwig organ, we eliminated this tissue by expressing the pro-apoptotic *hid* gene under the control of the *GMR* promoter (Hay et al., 1994). This manipulation was effective in eliminating the Bolwig organ, as previously reported (Xiang et al., 2010), since we did not detect anti-Rh6 staining in *GMR-hid* larvae (Figure 3B). The *GMR-hid* larvae showed temperature preference behavior similar to that of control animals (Figure 3C), indicating that Rh5 and Rh6 expression in the Bolwig organ was dispensable for thermotaxis in late third-instar larvae.

Because elimination of Rh5 or Rh6 disrupts signaling in the Bolwig organ, it was possible that the altered function of the photoreceptor cells in the Bolwig organ was disrupting thermotaxis behavior. If so, then elimination of the Bolwig organ might suppress the *rh5* or *rh6* mutant phenotypes. To test this possibility, we generated *GMR-hid* larvae carrying either the *rh5*^{G} or *rh6*^{G} mutations. We found that *GMR-hid,rh5*^{G} and *GMR-hid;rh6*^{G} flies displayed defects in 18°C selection (Figure 3C) similar to the rhodopsin mutants (Figure 2B). The *GMR-hid* transgene alone or *GMR-hid* in combination with the *rh5*^{G}/+ or *rh6*^{G}/+ heterozygous backgrounds had no effect on thermotaxis, as these animals showed normal 18°C preference similar to control larvae (Figure 3C). Therefore, elimination of the Bolwig organ did not suppress the *rh5*^{G} or *rh6*^{G} thermotaxis phenotypes.

rh5 and *rh6* Required in *trpA1* Neurons for Optimal Temperature Selection

The preceding data indicated that *rh5* and *rh6* functioned in thermotaxis through cells external to the Bolwig organ. To address the cellular requirements for *rh5* and *rh6*, we inactivated a variety of neurons by expressing *kir2.1* (*UAS-kir2.1*) under control of the *GAL4-UAS* system. Introduction of *kir2.1* in *rh5*- or *rh6*-expressing neurons using the *rh5*^{G}/+ and *rh6*^{G}/+ *GAL4*s decreased the proportion of larvae attracted to the 18°C zone (Figure 3D). The *GAL4* drivers alone (*rh5*^{G}/+, *rh6*^{G}/+) had no impact on temperature selection (Figure S3A). In contrast, silencing Bolwig neurons with either the *trp-GAL4* (Petersen and Stowers, 2011) or the *GMR-GAL4* (Hay et al., 1994) did not change the preference for this temperature zone (Figure 3D). The chordotonal and terminal organs participate in discriminating 18°C from cooler temperatures (Kwon et al., 2010; Liu et al., 2003). Inactivation of neurons in these organs using the *iav-GAL4*, *Gr33a*^{GAL4}, and *Gr66a-GAL4* (Kwon et al., 2011; Kwon et al., 2010) to drive *UAS-kir2.1* did not impact on selection of the 18°C zone in the thermal gradient (Figure 3E). Thus, we conclude that the Bolwig, chordotonal, and terminal organs are all dispensable for late third-instar larvae to choose the optimal temperature.

A subset of *trpA1*-expressing neurons were candidates for requiring *rh5* and *rh6*, since mutation of *trpA1* prevented mid-third-instar larvae from discriminating 18°C from other temperatures in the comfortable range (Kwon et al., 2008). Thus, we considered whether *trpA1*-expressing neurons were required in the late third-instar larvae. There are at least four *trpA1* mRNA isoforms (Figure S3B). The *trpA1-A* and *trpA1-B* isoforms (*trpA1-AB*) are expressed under the control of one promoter, and *trpA1-C* and *trpA1-D* (*trpA1-CD*) are synthesized using a second promoter (Figure S3B). In addition, each pair of isoforms differs through alternative splicing. We found that when we drove *UAS-kir2.1* expression using the *trpA1-AB*^{G4}/+ or the *trpA1-CD*^{G4}/+ reporter, the larvae were impaired in selecting 18°C (Figure 3F). Introduction of the reporters alone (*trpA1-AB*^{G4}/+ or *trpA1-CD*^{G4}/+) had no impact on temperature selection (Figure S3A). The *trpA1-AB* and *trpA1-CD* mutations each include either *GAL4* or *LexA* reporters inserted at the site of the original translation start codons (Figure S3B). The *trpA1-AB* reporter was expressed predominately in the brain and, to a lesser extent, in the ventral nerve cord (VNC), whereas the *trpA1-CD* reporter stained multidendritic type IV neurons and external sensory organ neurons in the body wall, which extended axons to the VNC (Figures S3C and S3D) (Zhong et al., 2012). We found that a null mutation in *trpA1* (*trpA1*^{1}) eliminated the preference of late third-instar larvae for the 18°C zone (Figure 3G). In addition, mutation of *trpA1-AB* (*trpA1-AB*^{G4}) prevented 18°C selection, whereas mutation of *trpA1-CD* (*trpA1-CD*^{G4}) significantly impaired 18°C thermotaxis (Figure 3G). These results indicate strongly that *trpA1* neurons were required for 18°C preference during the late third-instar period.

Our results led us to test whether *rh5* and *rh6* were expressed in *trpA1*-expressing neurons. The *trpA1-CD-QF*

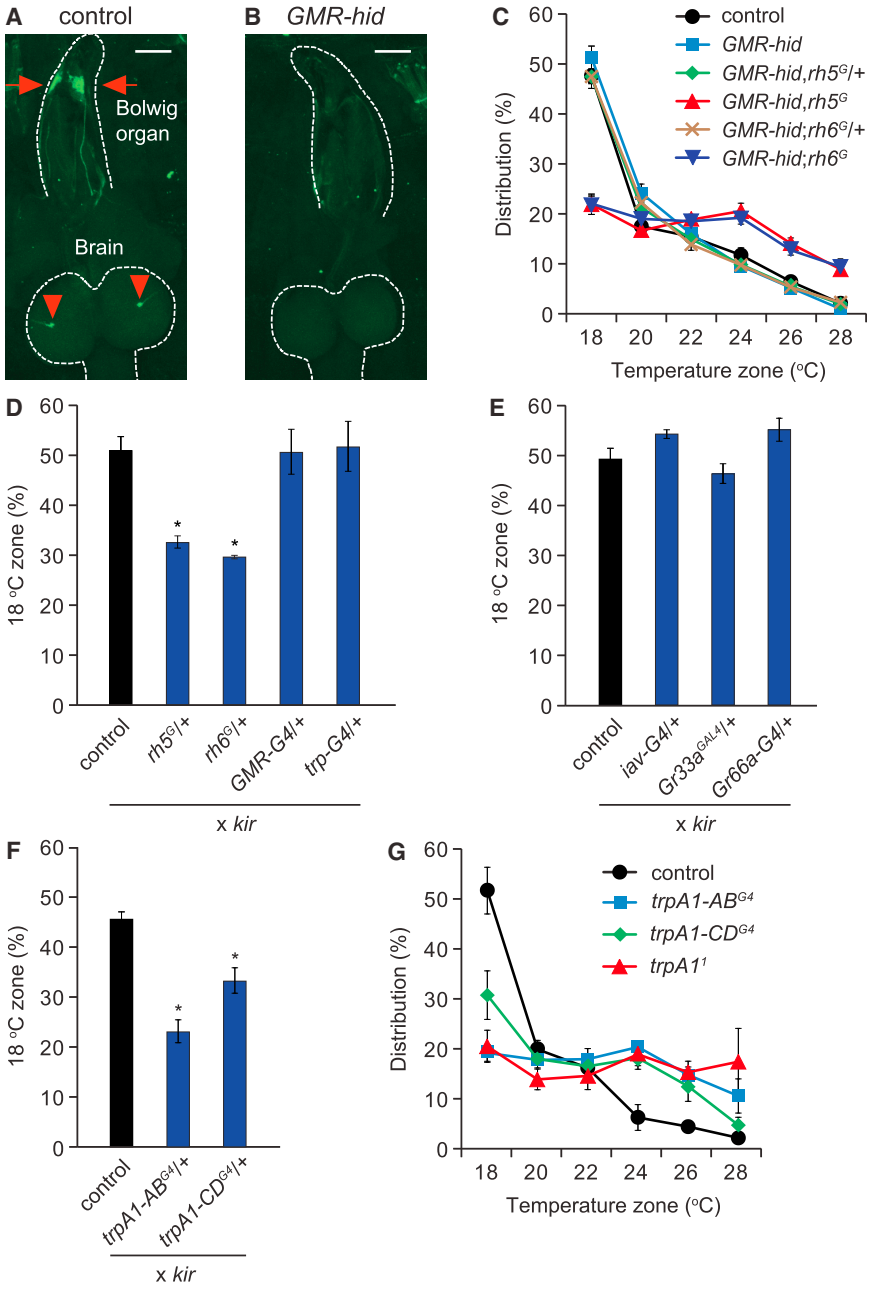

Figure 3. *rh5*- and *rh6*-Dependent Temperature Selection Depends on *trpA1* Neurons, but Not the Bolwig Organ

(A) Staining of control (w^{1118}) larvae with anti-Rh6. The antibodies labeled neurons in the Bolwig organ (arrows) and their processes that extend to the brain (arrowheads).

(B) Anti-Rh6 staining was not detectable after elimination of photoreceptor cells in the Bolwig organ with *GMR-hid*.

(C) Thermal preferences of control (w^{1118}), *GMR-hid*, and *GMR-hid* larvae carrying either the $rh5^G$ or $rh6^G$ mutations. n = 6–7.

(D–F) Fraction of larvae in the 18°C zone of an 18°C–28°C thermal gradient after expressing *UAS-kir* using the indicated *GAL4* lines. The control larvae harbored the *UAS-kir* (*UAS-kir*/+) transgene only. n = 4–5.

(G) Distribution of the indicated *trpA1* mutants in the six indicated temperature zones. n = 3–4.

Scale bars in (A) and (B) represent 100 μm. *p < 0.05 compared to the control. The error bars represent ± SEM. See also Figure S3.

reporter (Petersen and Stowers, 2011) drove expression of *QUAS-mCherry* in class IV neurons (ddaC and v'ada) and external sensory organ neuron vp5 (Figures 4A, 4D, and 4G)—an expression pattern consistent with the cellular distribution of the $trpA1\text{-}CD^{G4}$ reporter (Figures S3D and S4) (Zhong et al., 2012). Our initial attempts to detect *rh5* and *rh6* reporter expression in the body wall were unsuccessful. Therefore, we used *GAL4* reporters ($rh5^G$/+ and $rh6^G$/+) to drive two copies of a transgene encoding six tandem copies of *GFP* (*20XUAS-6XGFP*) and enhanced the signals using the tyramide signal amplification (TSA) method (Chao et al., 1996). We detected GFP signals driven by $rh5^G$/+ and $rh6^G$/+ (Figures 4B and 4E) that co-localized with the *trpA1-CD* staining (Figures 4C and 4F). We then wrote a script using MATLAB to automatically identify regions of interest (ROIs) based on the *trpA1-CD*-expressing cell bodies and to measure pixel intensities of the GFP signals. While the TSA approach resulted in some random background signals that occurred when using *UAS-GFP* only (Figures 4H and 4J), we detected significantly stronger signals in the presence of the $rh6^G$/+ reporter (ddac, v'ada, and vp5; Figures 4B and 4J). We also detected stronger signals in the same cells of larvae expressing the $rh5^G$/+ reporter. However, the increase in signal over background was statistically significant in vp5 only (Figures 4E and 4J). We also attempted to detect *rh5* and *rh6* reporter signals in *trpA1-AB* neurons, but this was impeded by high background staining in the brain and VNC when using the TSA approach. Nevertheless, the results with the *trpA1-CD* reporter indicate that *rh5* and *rh6* are co-expressed with *trpA1*.

Signaling Pathway Required for Thermotaxis in Late Third-Instar Larvae

To address whether *rh5*, *rh6*, and *trpA1* functioned in the same cells, we performed RNAi-mediated knockdown of *rh5* and *rh6* ($UAS\text{-}rh5^{RNAi}$ and $UAS\text{-}rh6^{RNAi}$), using a series of *GAL4* lines. Knockdown of either *rh5* or *rh6* using the *rh5*- or *rh6-GAL4* lines ($rh5^G$/+ and $rh6^G$/+, respectively) resulted in a significant reduction in 18°C selection (Figure 5A). We obtained similar reductions in larval distribution in the 18°C zone after suppressing either *rh5*

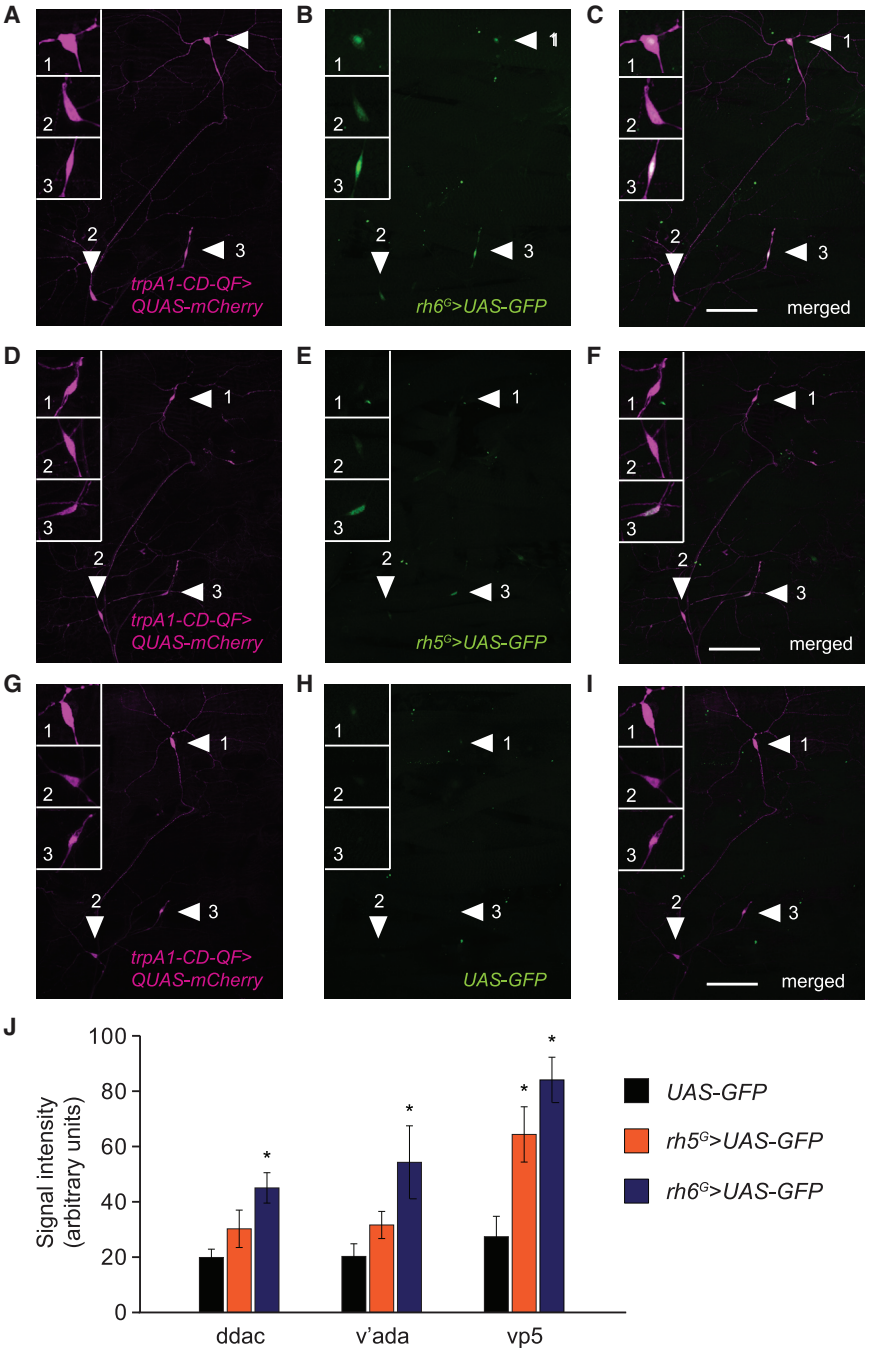

Figure 4. Co-expression of *rh5* and *rh6* with *trpA1* in the Body Wall

Representative confocal images of *rh5*, *rh6*, and *trpA1-CD* reporter expression from a third-instar larval body segment. The *rh5 GAL4* ($rh5^{G}$/+) and the *rh6 GAL4* ($rh6^{G}$/+) drove expression of two copies of *20XUAS-6XGFP* (*UAS-GFP*;anti-GFP, green). The *trpA1-CD* reporter (*trpA1-CD-QF*) drove expression of one copy of *mCherry* (*QUAS-mCherry*;anti-dsRed, magenta). The GFP signals were enhanced using the TSA approach. The arrowheads labeled 1, 2, and 3 indicate the cell bodies of *trpA1-CD*-positive neurons. Arrowheads 1 and 2 correspond to the type IV neurons ddaC and v'ada, and arrowhead 3 corresponds to the external sensory organ neuron vp5. The boxes labeled 1, 2, and 3 in the upper left of each panel show 3-fold magnifications of ddaC, v'ada, and vp5, respectively. See Figure S4 for depictions of the locations of the ddaC, v'ada, and vp5 neurons. In all pictures, the left is the anterior side and the top is the dorsal side.

(A–C) Co-expression of *rh6* and *trpA1-CD* reporters. (A) *trpA1-CD* reporter staining (*trpA1-CD-QF*/+;*QUAS-mCherry*/+). (B) *rh6* reporter staining (*20XUAS-6XGFP*/+;$rh6^{G}$,*20XUAS-6XGFP*/+). (C) Merge of (A) and (B).

(D–F) Co-expression of *rh5* and *trpA1-CD* reporters. (D) *trpA1-CD* reporter staining (*trpA1-CD-QF*/+;*QUAS-mCherry*/+). (E) *rh5* reporter staining ($rh5^{G}$,*20XUAS-6XGFP*/+;*20XUAS-6XGFP*/+). (F) Merge of (D) and (E).

(G–I) Control showing typical background staining in flies harboring the *UAS-GFP* transgene without a *GAL4* driver line. (G) *trpA1-CD* reporter staining (*trpA1-CD-QF*/+;*QUAS-mCherry*/+). (H) *UAS-GFP* only (*20XUAS-6XGFP*/+;*20XUAS-6XGFP*/+). (I) Merge of (G) and (H).

(J) Quantification of the GFP signals in the body wall neurons driven by *rh5* (orange) or *rh6* (blue) reporter or by *UAS-GFP* only (black). The ROIs were identified, and quantifications were performed automatically in an unbiased fashion using a MATLAB program. n = 9–11.

Scale bars in (C), (F), and (I) represent 100 μm. *$p < 0.05$ compared to the *UAS-GFP* control. The error bars represent ± SEM. See also Figure S4.

or *rh6* under control of $trpA1\text{-}AB^{G4}$ or $trpA1\text{-}CD^{G4}$ ($trpA1\text{-}AB^{G4}$/+ or $trpA1\text{-}CD^{G4}$/+; Figure 5A). Conversely, there were no significant effects resulting from RNAi-mediated knockdown of *rh5* or *rh6* using *GAL4* lines expressed in the Bolwig organ (*trp-GAL4*) or the mushroom bodies (*117Y-GAL4*; Figure 5A).

We also performed RNAi-mediated knockdown of *trpA1* using the *rh5*- and *rh6-GAL4* drivers. Knockdown of *trpA1* (*UAS-*$trpA1^{RNAi}$), using either the $rh5^{G}$ or $rh6^{G}$ ($rh5^{G}$/+ or $rh6^{G}$/+), resulted in a significant reduction in 18°C selection, which was similar to $trpA1\text{-}AB^{G4}$/+ and $trpA1\text{-}CD^{G4}$/+-induced *trpA1* knockdown (Figure 5B). RNAi-mediated knockdown of *trpA1* using the *trp-GAL4*, which is expressed in the Bolwig organ (Petersen and Stowers, 2011), had no effect (Figure 5B). Moreover, we performed rescue experiments focusing on *rh6* and found that the $rh6^{1}$ phenotype was suppressed by expression of *rh6* in combination with both the $trpA1\text{-}AB^{G4}$/+ and $trpA1\text{-}CD^{G4}$/+ drivers (Figure 5C). However, the rescue was reduced when we expressed *rh6* in *trpA1-AB* neurons alone, and there was no suppression resulting from *rh6* expression in *trpA1-CD* neurons alone (Figure 5C). The combination of these results indicate that *rh5* and *rh6* function together in 18°C temperature selection in *trpA1* neurons.

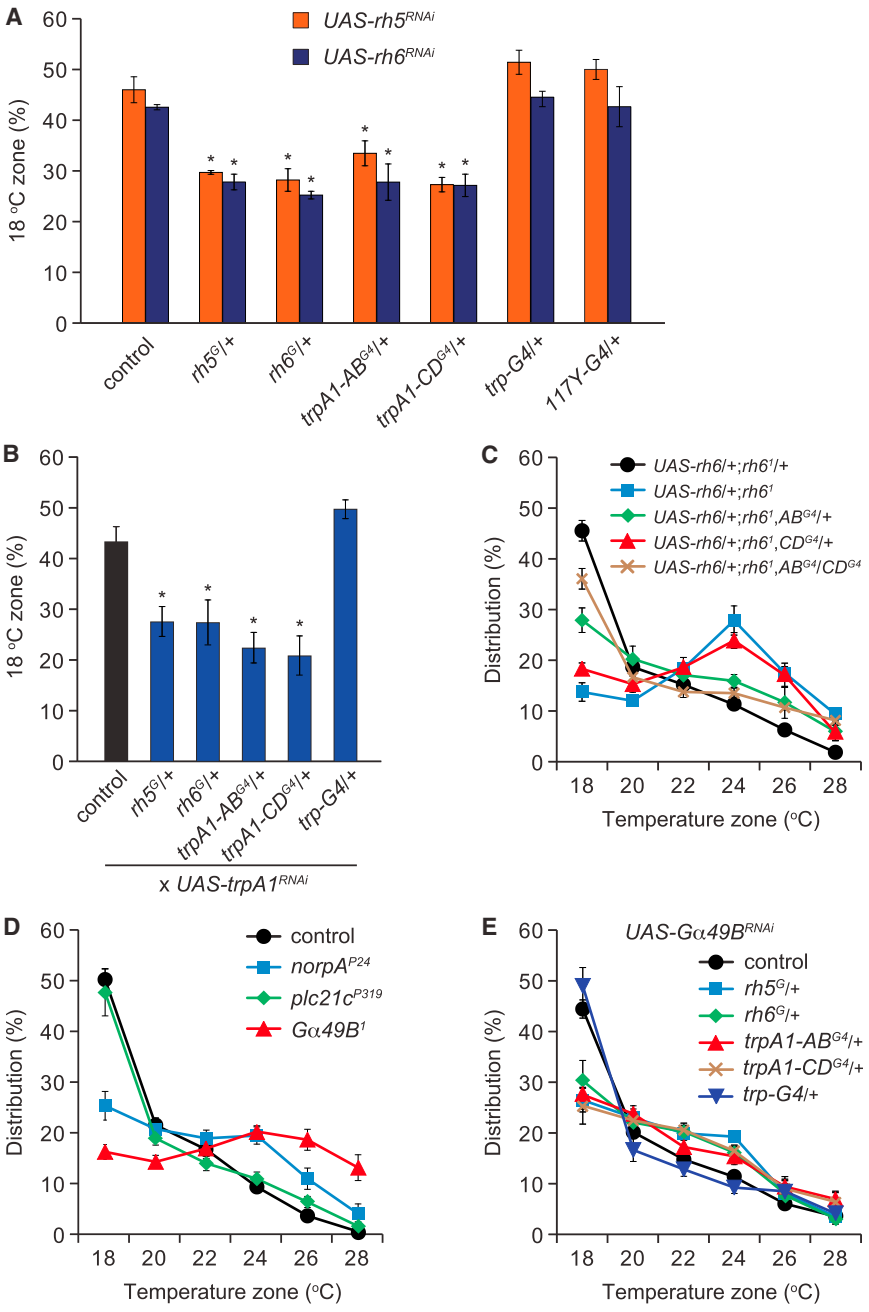

Figure 5. Requirements for *rh5*, *rh6*, *norpA*, and *Gα49B* in *trpA1* Neurons for Thermotaxis

Larvae of the indicated genotypes were assayed on 18°C–28°C thermal gradients.

(A) Percentages of larvae expressing *UAS-rh5^{RNAi}* (orange) or *UAS-rh6^{RNAi}* (blue) transgenes under control of the indicated *GAL4* lines in the 18°C zone. n = 5–7.

(B) Percentages of larvae expressing *dicer2;UAS-trpA1^{RNAi}* under control of the indicated *GAL4* lines in the 18°C zone. n = 4–5.

(C) Testing for rescue of the *rh6^{1}* mutant phenotype by expressing *UAS-rh6* under control of *trpA1-AB^{G4}* (*AB^{G4}*/+), *trpA1-CD^{G4}* (*CD^{G4}*/+) or both *GAL4*s (*AB^{G4}/CD^{G4}*). n = 5–6.

(D) Assaying thermotactic behavior of *plc* mutants (*norpA^{P24}* and *plc21c^{P319}*) and the *Gqα* mutant (*Gα49B^{1}*). n = 4–6.

(E) Thermal distribution of larvae expressing *UAS-Gα49B^{RNAi}* under control of the indicated *GAL4* lines. n = 4–6.

*p < 0.05 compared to the control. The error bars represent ± SEM. See also Figure S5.

To address whether the rhodopsin mutations affected the gross morphology of *trpA1-CD* neurons, we compared the appearance of the peripheral neurons expressing the *trpA1-CD* reporter in control and *rh5* and *rh6* mutant larvae. We found that the morphology of *trpA1-CD* neurons was indistinguishable in the mutants and heterozygous animals (Figures S5A–S5D). To test the possibility that the temperature preference phenotypes exhibited by the *rh5* and *rh6* mutants might be caused by a general deficit in thermotaxis or locomotor defects, we performed additional controls. We found that, when the larvae were given a choice between 18°C and 28°C, the *rh5* and *rh6* mutants avoided 28°C and accumulated on the 18°C side, similarly to control larvae (Figure S5E). These latter results suggest that the deficits in temperature selection exhibited by the rhodopsin mutants were not due to general impairment in thermotaxis or reductions in locomotor activities. In further support of this latter conclusion, the moving speeds of the *rh5* and *rh6* mutant larvae were comparable to the control, except for a slight elevation in the *rh6^{G}* allele (Figure S5F).

Drosophila rhodopsins couple to a Gq/phospholipase Cβ (PLC)/TRP channel signaling cascade in photoreceptor cells (Montell, 2012). Moreover, we showed previously that Rh1 functions in thermotaxis during the mid-third-instar larval period in collaboration with a Gq/PLC/TRPA1 signaling cascade (Kwon et al., 2008; Shen et al., 2011). *Drosophila* encodes one Gqα (*Gα49B*) and two PLCs (NORPA and PLC21c). We found that late third-instar larvae carrying either the *Gα49B^{1}* or *norpA^{P24}* mutation exhibited defects in 18°C thermotaxis, whereas the behavior of *plc21C^{P319}* mutant larvae was indistinguishable from controls (Figure 5D). We also observed a thermotaxis defect resulting from RNAi-mediated knockdown of *Gα49B* using *GAL4* lines that directed expression in *rh5*, *rh6*, *trpA1-AB*, or *trpA1-CD* neurons (Figure 5E).

DISCUSSION

We conclude that third-instar *Drosophila* larvae undergo an age-dependent change in their thermal preference, and this behavioral

modification requires several rhodopsins. Rh5 and Rh6 were the most important, given that the stage-dependent alteration in temperature selection was eliminated in either *rh5* and *rh6* mutant flies. Several observations support the conclusion that the thermotaxis phenotypes exhibited by the *rh5* and *rh6* mutants are not secondary consequences of developmental defects or motor problems. We found that the percentage of larvae that entered the third-instar larval stage at 74 hr AEL were similar to controls, as were the times to pupation. Furthermore, the morphology of the peripheral *trpA1*-positive neurons that normally express *rh5* and *rh6* were indistinguishable between the *rh5* and *rh6* mutants and controls. In addition, the movement speeds of the *rh5* and *rh6* mutants were not reduced, and they were able to choose 18°C over 28°C normally in two-way choice assays.

The requirements for Rh5 and Rh6 were light independent, since the thermotaxis occurred equally well in the light or dark and was not dependent on the Bolwig organ, which is the rhodopsin-expressing light-sensitive tissue in larvae. Rhodopsins are composed of the protein subunit, opsin, and a vitamin-A-derived chromophore, which senses light. In *Drosophila* photoreceptor cells, the chromophore also functions as a molecular chaperone to facilitate transport of the opsin out of the endoplasmic reticulum (Ozaki et al., 1993). We found that thermotaxis in late third-instar larvae was impaired in a mutant that disrupts chromophore biosynthesis. However, we suggest that this phenotype is due to the second function of the chromophore as a molecular chaperone.

Our findings lead us to conclude that Rh5 and Rh6 function upstream of a Gq/PLC/TRPA1 signaling cascade, which allows late third-instar larvae to select their favorite temperature in the comfortable range. We propose that this pathway enables the animals to sense minute temperature differences over a shallow thermal gradient through signal amplification, similar to the role of these proteins in phototransduction. If the perfect option is not available in the thermal landscape, the thermosensory signaling cascade may facilitate adaptation to hospitable temperatures that deviate slightly from their preferred temperature.

Because of the exquisite effectiveness of rhodopsin in photon capture, we suggest that Rh5 and Rh6 are expressed outside the Bolwig organ at extremely low levels to prevent light from interfering with temperature sensation. Nevertheless, we detected expression of the *rh5* and *rh6* reporters in a subset of *trpA1-CD* neurons in the body wall. Using the *GAL4/UAS* system, we provided evidence that *rh5* and *rh6* both function in *trpA1-CD*- as well as *trpA1-AB*-expressing neurons outside of the Bolwig organ. In addition, *rh5 GAL4*-mediated RNAi knockdown of *rh6* and *rh6 GAL4*-mediated knockdown of *rh5* resulted in defects in 18°C selection. RNAi-based knockdown of *trpA1* with either of the *rh5*- and *rh6-GAL4* drivers caused similar thermotaxis defects. Although these drivers are expressed at very low levels, we suggest that they are still effective, since *trpA1* is also expressed at very low levels in the periphery (Xiang et al., 2010). The effects of the *rh5*- and *rh6-GAL4* drivers in suppressing *trpA1* were not non-specific, as we did not observe a thermotaxis phenotype using the *trp-GAL4* driver. We also found that the *rh5*- and *rh6-GAL4*s silenced the thermosensory neurons in combination with *UAS-kir2.1*. We propose that this was effective, since small increases in hyperpolarization due to slight elevation of Kir2.1 cannot be overcome by the slight depolarization mediated by the low levels of TRPA1.

The combination of these findings indicates that both *rh5* and *rh6* are co-expressed and function in the same, or overlapping, subsets of neurons required for thermotaxis. These findings raise the possibility that Rh5 and Rh6 may form heterodimers in vivo. Another key question is whether rhodopsins are direct thermosensors, an issue that remains unresolved due to challenges inherent in expressing these and most invertebrate rhodopsins in vitro.

The observation that multiple rhodopsins function in thermotaxis in *Drosophila* raise the question as to whether rhodopsin-dependent thermosensory signaling cascades are used in other animals, including mammals. We suggest that mammalian cells that undergo thermotaxis over very small temperature gradients may rely on opsin-coupled amplification cascades. Intriguing possibilities include leukocytes, which thermotax to sites of inflammation (Kessler et al., 1979), and mammalian sperm, which undergo thermotaxis to the egg over temperature gradients of ~1°C and require PLC for this cellular behavior (Bahat and Eisenbach, 2010; Bahat et al., 2003). Intriguingly, mammalian TRP channels and non-visual rhodopsins appear to be expressed in sperm and have been suggested to function in sperm thermotaxis (Kumar and Shoeb, 2011; Kumbalasiri and Provencio, 2005; Pérez-Cerezales et al., 2015).

EXPERIMENTAL PROCEDURES

Generation of *rh5^G and rh6^G* Flies

We generated *rh5^G* and *rh6 ^{G}* by ends-out homologous recombination (Gong and Golic, 2003).

Temperature Gradient Assays

We reared the larvae under standard 12-hr/12-hr light/dark cycles. We prepared synchronized larvae and assayed the distribution of ~150 larvae on linear 18°C–28°C continuous gradients after allowing them to explore for 11–20 min, depending on their age. We tabulated the larvae in each of the six temperature zones and calculated the distribution as follows: (number of larvae in a given 2-cm zone)/(total number of larvae in six zones) × 100%.

Evaluation of Developmental Rate

The percentages of pupae were calculated based on the maximum number at 227 hr AEL. T_{50} and T_{80} were the times at which 50% and 80% of the animals underwent pupation, respectively.

Immunostaining

To perform immunostaining, third-instar larvae were dissected and stained, followed, in some cases, by signal amplification using the TSA method. Samples were imaged using a Zeiss LSM 700 confocal laser scanning microscope and a 20×/0.8 Plan-Apochromat DIC (differential interference contrast) objective. The images were analyzed using Zen software.

Statistics

Multiple comparisons between the wild-type control and test groups were performed using one-way ANOVA, followed by Dunnett's post hoc test. Values are shown as mean ± SEM, unless indicated otherwise. A p value <0.05 was considered significant.

SUPPLEMENTAL INFORMATION

Supplemental Information includes Supplemental Experimental Procedures and five figures and can be found with this article online at http://dx.doi.org/10.1016/j.celrep.2016.09.028.

AUTHOR CONTRIBUTIONS

T.S., H.-C.C., and C.M. designed the study, analyzed the data, and wrote the manuscript. T.S. and H.-C.C. performed most of the experiments. J.L. prepared MATLAB programs for performing and quantifying immunostaining and larval locomotion. H.-C.C. generated the *rh5*^{G} and *rh6*^{G} mutants, and J.L. generated the *trpA1-AB*^{LexA} *and trpA1-CD*^{G4} mutants.

ACKNOWLEDGMENTS

This work was supported by a grant to C.M. from the National Eye Institute (EY008117).

Received: September 9, 2015
Revised: July 18, 2016
Accepted: September 8, 2016
Published: October 4, 2016

REFERENCES

Bahat, A., and Eisenbach, M. (2010). Human sperm thermotaxis is mediated by phospholipase C and inositol trisphosphate receptor Ca^{2+} channel. Biol. Reprod. *82*, 606–616.

Bahat, A., Tur-Kaspa, I., Gakamsky, A., Giojalas, L.C., Breitbart, H., and Eisenbach, M. (2003). Thermotaxis of mammalian sperm cells: a potential navigation mechanism in the female genital tract. Nat. Med. *9*, 149–150.

Chao, J., DeBiasio, R., Zhu, Z., Giuliano, K.A., and Schmidt, B.F. (1996). Immunofluorescence signal amplification by the enzyme-catalyzed deposition of a fluorescent reporter substrate (CARD). Cytometry *23*, 48–53.

Fowler, M.A., and Montell, C. (2013). *Drosophila* TRP channels and animal behavior. Life Sci. *92*, 394–403.

Gong, W.J., and Golic, K.G. (2003). Ends-out, or replacement, gene targeting in *Drosophila*. Proc. Natl. Acad. Sci. USA *100*, 2556–2561.

Hay, B.A., Wolff, T., and Rubin, G.M. (1994). Expression of baculovirus P35 prevents cell death in *Drosophila*. Development *120*, 2121–2129.

Julius, D. (2013). TRP channels and pain. Annu. Rev. Cell Dev. Biol. *29*, 355–384.

Kessler, J.O., Jarvik, L.F., Fu, T.K., and Matsuyama, S.S. (1979). Thermotaxis, chemotaxis and age. Age *2*, 5–11.

Klein, M., Afonso, B., Vonner, A.J., Hernandez-Nunez, L., Berck, M., Tabone, C.J., Kane, E.A., Pieribone, V.A., Nitabach, M.N., Cardona, A., et al. (2015). Sensory determinants of behavioral dynamics in *Drosophila* thermotaxis. Proc. Natl. Acad. Sci. USA *112*, E220–E229.

Kumar, P.G., and Shoeb, M. (2011). The role of trp ion channels in testicular function. Adv. Exp. Med. Biol. *704*, 881–908.

Kumbalasiri, T., and Provencio, I. (2005). Melanopsin and other novel mammalian opsins. Exp. Eye Res. *81*, 368–375.

Kwon, Y., Shim, H.S., Wang, X., and Montell, C. (2008). Control of thermotactic behavior via coupling of a TRP channel to a phospholipase C signaling cascade. Nat. Neurosci. *11*, 871–873.

Kwon, Y., Shen, W.L., Shim, H.S., and Montell, C. (2010). Fine thermotactic discrimination between the optimal and slightly cooler temperatures via a TRPV channel in chordotonal neurons. J. Neurosci. *30*, 10465–10471.

Kwon, J.Y., Dahanukar, A., Weiss, L.A., and Carlson, J.R. (2011). Molecular and cellular organization of the taste system in the *Drosophila* larva. J. Neurosci. *31*, 15300–15309.

Liu, L., Yermolaieva, O., Johnson, W.A., Abboud, F.M., and Welsh, M.J. (2003). Identification and function of thermosensory neurons in *Drosophila* larvae. Nat. Neurosci. *6*, 267–273.

Mazzoni, E.O., Desplan, C., and Blau, J. (2005). Circadian pacemaker neurons transmit and modulate visual information to control a rapid behavioral response. Neuron *45*, 293–300.

Montell, C. (2012). *Drosophila* visual transduction. Trends Neurosci. *35*, 356–363.

Ozaki, K., Nagatani, H., Ozaki, M., and Tokunaga, F. (1993). Maturation of major Drosophila rhodopsin, ninaE, requires chromophore 3-hydroxyretinal. Neuron *10*, 1113–1119.

Pérez-Cerezales, S., Boryshpolets, S., Afanzar, O., Brandis, A., Nevo, R., Kiss, V., and Eisenbach, M. (2015). Involvement of opsins in mammalian sperm thermotaxis. Sci. Rep. *5*, 16146.

Petersen, L.K., and Stowers, R.S. (2011). A Gateway MultiSite recombination cloning toolkit. PLoS ONE *6*, e24531.

Shen, W.L., Kwon, Y., Adegbola, A.A., Luo, J., Chess, A., and Montell, C. (2011). Function of rhodopsin in temperature discrimination in *Drosophila*. Science *331*, 1333–1336.

Sprecher, S.G., Pichaud, F., and Desplan, C. (2007). Adult and larval photoreceptors use different mechanisms to specify the same Rhodopsin fates. Genes Dev. *21*, 2182–2195.

Venkatachalam, K., and Montell, C. (2007). TRP channels. Annu. Rev. Biochem. *76*, 387–417.

Venkatachalam, K., Luo, J., and Montell, C. (2014). Evolutionarily conserved, multitasking TRP channels: lessons from worms and flies. Handbook Exp. Pharmacol. *223*, 937–962.

Wang, T., Jiao, Y., and Montell, C. (2007). Dissection of the pathway required for generation of vitamin A and for *Drosophila* phototransduction. J. Cell Biol. *177*, 305–316.

Wu, Q., Wen, T., Lee, G., Park, J.H., Cai, H.N., and Shen, P. (2003). Developmental control of foraging and social behavior by the *Drosophila* neuropeptide Y-like system. Neuron *39*, 147–161.

Xiang, Y., Yuan, Q., Vogt, N., Looger, L.L., Jan, L.Y., and Jan, Y.N. (2010). Light-avoidance-mediating photoreceptors tile the *Drosophila* larval body wall. Nature *468*, 921–926.

Zhong, L., Bellemer, A., Yan, H., Ken, H., Jessica, R., Hwang, R.Y., Pitt, G.S., and Tracey, W.D. (2012). Thermosensory and nonthermosensory isoforms of *Drosophila melanogaster* TRPA1 reveal heat-sensor domains of a thermoTRP Channel. Cell Rep. *1*, 43–55.